A long duration cryostat suitable for balloon borne photometry

S. Masi[1], P. Cardoni[2], P. de Bernardis[1]
F. Piacentini[1], A. Raccanelli[1], F. Scaramuzzi[2]

[1] Dipartimento di Fisica, Universita' La Sapienza, Roma, Italy
[2] ENEA-CRE, Frascati, Italy

Abstract

We describe a ^{4}He cryostat suitable for cooling a large (about 50 liters in volume) multiband bolometric photometer for mm-waves. The cryostat features two large optical windows and a hold time longer than two weeks. The long hold time has been obtained using a 20K vapor cooled shield for the liquid He tank and superinsulation for the nitrogen tank. The tanks are supported by kevlar cords. The cryostat has been optimized for operation on long duration stratospheric balloon flights, and has been tested successfully at ground and in two short balloon flights.

Oct.15, 1998. Submitted to **Cryogenics**.

1. Introduction

BOOMERanG is an experiment devoted to map the Cosmic Microwave Background (CMB) with very high sensitivity (typically 10 - 20 μK per pixel) and angular resolution (12 - 20 arcmin FWHM) (see Lange *et al*[1], de Bernardis *et al*[2], Masi *et al*[3]). The program is a set of 2 balloon flights: BOOMERanG North America (August 1997), BOOMERanG Long Duration Balloon (December 1998).

A custom cryostat has been developed to mantain the bolometric detectors, the first stage of signal amplification, the reimaging optics and the optical filters at cryogenic temperatures for the two weeks of the long duration balloon flight. A ^{3}He fridge, used to cool the detectors at 0.28K during the flight, is described elsewhere[6]. Here we describe the main ^{4}He dewar.

Our group has already developed He cryostats for balloon-borne mm-wave photometers, like the ARGO one[7]. However, the BOOMERanG experiment is quite different, since there is a need for extendend hold time (two weeks or more for the flights carried out by NASA-NSBF around Antarctica) and more severe mechanical strength specifications (all the mechanical components on the payload must be able to withstand accelerations as large as $10g$ on the vertical and $5g$ at 45 degrees from the vertical).

Moreover, the BOOMERanG cryogenic focal plane assembly is significantly larger and heavier than the ARGO one. The volume of the experimental insert, which includes the reimaging optics, the multiband photometers, the cold preamplifiers and the ^{3}He fridge, is a cylinder of 0.32 m diameter and 0.64 m height. These dimensions, together with the required hold time, drive the large dimensions of the cryostat.

In fact, in order to surround the experimental insert, the surface area of the helium tank cannot be smaller than 1.5 m^2. This means that the radiative heat input on the helium bath from a 77K graybody, assuming 8% emissivities, is larger than 80 mW. This produces a helium boiloff larger than 2 liters/day for a pumped helium bath. For a 20 days hold time this would require an initial volume of 60 liters of liquid helium (which are reduced to about half after pumpdown). Since we have additional heat loads from the mechanical suspension system, from the bolometer preamplifiers, from the fill/vent lines, and from the optical windows, we need to reduce significantly this radiative heat load. We decided to mantain a 60 liters volume for the helium tank, and use a vapour cooled shield in between the helium tank and the nitrogen tank.

A similar computation can be done for the Nitrogen tank: the result is that we need a very good system for shielding radiation from the 300K shell. Using a superinsulation blanket it is possible to reduce the heat load from 300K radiation from over ~ 20 W/m^2 down to ~ 1 W/m^2 ([8]). Since the exposed surface area of the nitrogen tank is going to be about 3 m^2, we need about 60 liters of liquid nitrogen for a 20 days hold time.

2. Cryostat Design

The baselines for the cryostat design were:

1) Evaporation cryostat with liquid nitrogen and liquid helium. This solution is simple, reliable and cheap. Has the disadvantage of requiring a significant volume for storage of the liquids and a significant mass, especially for the Nitrogen tank. Active cooler solutions have been discarded for tho reasons: the power available on the staratospheric

payload is limited, and the bolometric detectors, which are usually microphonic, require a vibration-free environment.

2) Toroidal geometry of the He and N tanks as in the ARGO cryostat[7]. This solution features a large isothermal cold volume for the experimental insert. The thermal and mechanical interface for the experimental insert is a bolt circle on the bottom flange of the helium tank. In this way the insert can be easily introduced or removed from the cryostat, opening only the bottom cover of the cryostat.

3) The tanks are made from 6061 aluminum alloy to reduce the cryostat weigth. The filling and vent lines are made using stainless steel bellows to minimize heat conduction. The filling / vent lines are connected to the cryogen tanks by means of explosion weld stainless steel to aluminum joints. This solution has been used successfully in other liquid helium cryostats[9,7].

4) The tanks are supported by a web of kevlar cord straps. The significant weight of the tanks and of the experimental insert does not allow the use of the vent / fill lines as mechanical supports for the tanks. Kevlar cords have been used succesfully as cryogenic supports in smaller systems[10,11]. In fact tensioned Kevlar cords feature a stiffness to thermal conductivity ratio about 10 times larger than stainless steel cables. An alternative solution, the use of fiberglass cylinders concentric to the tanks, does not produce significant advantages in terms of resonance frequencies of the system, and makes the access to the different stages of the cryostat more difficult[12].

5) The radiative heat load on the Helium tank is reduced by means of an intermediate temperature shield. The shield is actively cooled by the helium evaporating from the He tank. This is a standard choice for storage cryostats[13,14,15], cryostats for space missions[16,17], and stratospheric balloon experiments[18].

6) The radiative heat load on the nitrogen tank is reduced by means of a multilayer aluminized mylar superinsulation (MLI). This is also standard practice (see e.g. [19,20,21]). The main problems are to build a MLI which can be very well evacuated, not compressed, and to avoid radiation leaks along the fill / vent tubes and support structures as well as in the optical path of the photometer. Due to the web structure of the supports, this is especially complex in our cryostat.

7) The size of the optical window must be minimized to withstand atmospheric pressure with a very thin, low emissivity, layer of polypropylene (50 μm). For this reason the window is mounted on a re-entrant funnel on the lower flange of the cryostat, so that the window is as close as possible to the focus of the internal optical system. The system has two optical windows, each 76 mm in diameter.

3. Cryostat development and optimization

A section of the cryostat is shown in fig.1. The main specifications are listed in table 1.

3.1 Suspension System

We used 1.65 mm diameter kevlar ropes[22], as shown in fig.2A, where the He tank with its suspension system is sketched. Kevlar must be pre-tensioned because it has a negative thermal expansion coefficient. Also, we need a tensioning mechanism easy to access and simple to operate, to allow for iterative re-tensioning after first installation. For each cryogen tank we have a kevlar suspension both on the top and on the bottom of the tank. The tensioning system is shown in fig.2B. A single kevlar cord runs through smooth eyebolts (E in fig.2B) mounted on two rings. The first ring (R1) is directly attached to the cryogen tank, while the second ring (R2) has adjustable height and is connected to the higher temperature stage. This adjustable ring is mounted using long screws (S) and stacks of Belleville conical washers (W). Kevlar is installed with the washers fully compressed by the screws. The two ends of the rope are coiled several times around the smooth surface of the first eyebolt, a couple of simple knots are made, and mylar tape is used to block them. After installation, kevlar can be tensioned simply undoing all the screws in the ring. The washers act as springs, mantaining optimal tensioning of the kevlar cords against natural and thermal kevlar expansion and against vacuum contraction of the outer shell. After first installation, a single re-tensioning after 24 hours is enough to produce long term tension of the system. Using 16 washers, the system can compensate a play as large as 2 mm in height, or 50 mm in length of the kevlar rope. The tension of the rope can be estimated by measuring the vibration frequency of the cord sections in between eyebolts. With this method we adjust the tension to 10-20 daN (depending on the tank and on the location - upper or lower). These values of tension produce vibrations in the range 100-200 Hz.

We made a set of breaking tests [23] on samples of this Kevlar rope. The breaking strenght of the Kevlar rope itself is around 300 daN, but in the knots the breaking strength is reduced to about 140 daN. With a suspended weight of about 70 Kg these measurements guarantee a large safety factor in normal conditions and still a good one at the 10g parachute opening shock.

Our support system has a number of resonance vibration modes. These vibrations could be excited by the payload scan during the observations. This could in principle induce spurious signals in the detectors, due to both microphonics and to the relative movement of several stops in the optical path of the system. So one has to be sure that the resonance vibrations either have frequencies higher than the highest frequency in the signal bandwidth (about 20 Hz in the case of the BOOMERanG experiment) or have negligible amplitude. The resonance frequencies have been checked using a numerical structural analysis model[12], and are in the range 10 - 100 Hz. These frequencies are not easily excited by the azimuth scan, which is at much lower frequency ($\sim 16mHz$). For the Helium tank, the main mode excited by our azimuth scan is the rotation around the vertical axis: the frequency is

$$f_\alpha \sim \frac{1}{2\pi}\sqrt{\frac{Nr^2k}{I}}$$

where $N = 24$ is the number of kevlar ropes, r is the radius of the suspended mass with inertia moment I, and $k \sim 4 \times 10^5\ N/m$ is the spring constant of each kevlar rope. We get $f_\alpha \sim 51Hz$ for our dewar. We have computed the motion of the inner part of the dewar when the outer shell is driven by the payload pointing system in a smoothed triangle-wave azimuth scan, 50^o wide, with a period of 1 minute and a 95% duty cycle. The most important factor in the analysis is the damping time of the induced vibrations. Vibration energy damping is due to friction between the different fibers of the springs. Since we are using braided kevlar cords we get a damping time relatively short, of the order of few seconds. We find that this azimuth mode is excited only during the scan turnarounds, with a maximum amplitude of 2 arcmin peak to peak. In the worst case, we can imagine the detectors looking to a cold stop in the 10 % sidelobe of the beam, vibrating against the sky background at balloon altitude. The brightness variation induced by this effect in our mm band is equivalent to a CMB anisotropy smaller than 10 μK, and is outside the useful signal bandwidth defined by our scan strategy.

3.2 Superinsulation

The Nitrogen tank has a large surface area (about 2.7 m^2) so that the dominant heat load is radiation from the 300K shell. We reduced it in two ways. First we surrounded the nitrogen tank and the inner part of the external shell with a low emissivity aluminum foil; second, we mounted a multilayer superinsulation in aluminized mylar in the space between the outer shell and the N tank. Using the standard formula[19] for radiative heat transmission between two surfaces A_1 and A_2 at temperatures T_1 and T_2 ($> T_1$), for n layers of superinsulation with aluminum on one side and a thermal insulator on the other, assuming $A_i = A$ for each surface i and $\epsilon_{Al} \ll 1$ we get

$$\dot{Q}_{rad} = \frac{\epsilon_{Al}}{n+1} A\sigma (T_{n+1}^4 - T_0^4)$$

Using this formula we find that the minimum number of layers required to obtain our $1 W/m^2$ goal is $n \sim 30$. We surrounded the tank with a blanket made from Cryolam [24], featuring built-in fiber spacer layers. To make evacuation easier, each layer of mylar was perforated making star-shaped cuts, with a random pattern and a density of $\sim 600 m^{-2}$. Care was taken for not to press the layers and for proper sealing of holes for kevlar cords, electrical wiring and fill/vent tubes. We divided the blanket in three parts: top, side, and bottom. Different parts are connected by interleaving adjacent corresponding layers. The side part is supported by the top part by means of velcro straps, and the same technique is used for attaching the bottom part to the side part. This blanket reduced the heat load on the Nitrogen tank by a factor 10. The measured evaporation rate is 0.15 liters of liquid per hour, corresponding to a 17 days hold time.

3.3 Vapor Cooled Shield

Helium vapors exit the He tank from the top, where a fill line and a vent line are present. The fill line is straight, to allow for Helium transfer, and is usually closed during cryostat operation. The vent line is used to convey cold vapours on the copper shield surrounding the He tank (S20K in fig.1), intercepting radiation from the 77K tank, and cooled by the enthalpy of the He vapours.

The shield is suspended by means of three thin wall stainless steel tubes (diameter 1.4 cm, thickness 0.3 mm, length 6.5 cm) on the top of the He tank, and by means of vespel / nylon spikes on the sides. In our system, we have a twin optical window (each 76 mm in diameter, W in fig.1) on the bottom cover of the cryostat, and an optical path (for radiation to be detected) up to the ^{3}He fridge, inside the experiment volume cooled by the He tank. Most of the spectrum of the incoming radiation is reflected or absorbed by means of suitable filters at 77K and 4.2K in the lower part of the dewar. For this reason we expect that the lower part of the shield could be warmer than the higher part. So we made two paths for the cold He vapours. The first one goes directly to a heat exchanger (EX in fig.1) on the top face of the shield. This is made with a copper cavity (diam. 130 mm, heigth 51 mm) divided into 7 sections. Cold gas enters the first section from the bottom and exits from the last section on the top, after a zigzag walk through subsequent sections. The second vent path is a copper tube serpentine (S in fig.1) soft welded to the bottom of the shield. The flow of vapours in the two circuits can be regulated by means of a valve mounted on the top part of the shield, and actuated by a small electrical motor. This allows us to optimize the performance and to fight the development of Taconis oscillations along the vent line. A diagram of the He plumbing inside the cryostat is shown in fig.3. The serpentine is 11 m long and 8 mm i.d. . We used a stainless steel bellows valve (V1 in fig.1, mod. Nupro SS-6BW) to regulate the flux of gas through the heat exchanger. The valve has been carefully cleaned from the grease with an ultrasonic cleaner to allow cryogenic operation. When the valve is completely closed, all the vapors are forced to pass through the serpentine. When the valve is fully open, most of the gas goes through the heat exchanger, due to the lower flow impedance. The valve is remotely controlled by means of a DC motor and a gearbox mounted on the shaft. The motor sleeve bearings have been rebored to allow low temperature operation. A custom gearbox with brass gears and sufficient play in the shaft has been used. We can read the valve position by means of a linear variable differential transformer (LVDT) detecting the position of the valve shaft. The presence of this valve allows us to set and trim the impedance of the circuit during pumpdown, and fighting Taconis oscillations (see section 3.5). After pumpdown, we can regulate the impedance, thus achieving the optimal temperature of the intermediate shield.

3.4 Heat Load Analysis

3.4.1: Helium Tank

The heat load on the Helium tank strongly depends on the temperature of the intermediate shield. The equilibrium temperature of the shield T_{sh} is the result of a balance between thermal input ($\dot{Q}_{ShIN}$) and cooling due to helium vapours:

$$\dot{Q}_{ShOUT} = -\dot{m} \int_{2K}^{T_{gas}} C_{He}(T) dT = -\dot{m}\epsilon \int_{2K}^{T_{sh}} C_{He}(T) dT \tag{1}$$

Where C_{He} is the specific heat of the Helium gas and T_{gas} is the temperature of the gas after exchanging with the shield with efficiency ϵ. The helium evaporation rate is $\dot{m} = \dot{Q}_{He}/L_{He}(2K)$ and $\dot{Q}_{He}$ depends on T_{sh}. At the eqilibrium we have

$$\dot{Q}_{ShOUT} + \dot{Q}_{ShIN} = 0 \tag{2}$$

The heat input is divided in conduction through the fill/vent tubes, (stainless steel bellows, 200μm thick, 12 mm diameter, 11 cm long, thermally anchored to the shield), conduction through the kevlar cords (20 mW), radiation from the shield, radiation dissipated in the optical filters and power dissipated in the experiment. Once all these heat loads are estimated, the only unknown in equation 2 is T_{sh}. We built a numerical code describing all the heat loads taking into account the geometrical and physical parameters of the dewar components. This code was used to solve numerically eq.2 to estimate the temperature of the shield and the thermal input on the helium bath. The code was extremely useful during optimization of the cryostat. The results for the final configuration of the dewar are listed in table 2 for different values of ϵ. For low efficiency ($\epsilon \sim 0.1$), the shield temperature is $\sim$ 50 K and the total heat load on the helium tank is $\sim$ 150 mW. For high efficiency $\epsilon \to 1$, we get a temperature of the shield $\sim 20K$ and a heat load on the He bath $\sim 50mW$. The measured evaporation rate depends on the conditions in which the cryostat works. We have data for three cases:

• Cryostat completely closed to outer radiation, without funnel (F in Fig.1); T_{He}=4.2 K: here the evaporation rate is 44 liters of gas per hour (STP), corresponding to 41 mW of heat load on the He (60 days of hold time, unpumped). The shield temperature is 22 K. Comparing these measurements with the predictions of the model (see table 2), we find that the exchange efficienciy is $\epsilon \sim 0.7$.

• Cryostat completely closed to the outer radiation, with funnel (not covered with superinsulation), 16 field effect transistors (FET) working as impedance adaptors for the bolometers (8 mW), the bath pumped down to T=2 K (32 liters of liquid remaining in the tank after pumpdown); the evaporation rate is 78 liters of gas per hour, corresponding to a heat load of 82 mW (14 days of hold time after pumpdown). The shield temperature is around 16 K.

• Window open, with filters on the funnel, 36 FETs working, T=2 K; in this case the evaporation rate is 110 liters of gas per hour, corresponding to a heat load of 100 mW (12 days of hold time after pumpdown). The shield temperature is around 10 K.

Most of the heat load with the window open (2nd and 3rd cases) is due to 300K thermal radiation leaking through the optical filters at 77 K. This will improve in flight, since the radiative background is expected to be much lower.

3.4.2: Nitrogen Tank

The total heat load from 300K through the superinsulation is a combination of radiative, conductive and convective thermal input and has been measured to be (5.1±0.3)W with no windows in the 300 K shell. The estimated heat load from the support kevlar ropes, the vent/fill lines and from the stainless steel signal cables is 0.75 W, so we get a total load through the superinsulation $\sim 1.6W/m^2$, close enough to the results of other experiments. Opening the large optical window and exposing the system to a 300K blackbody we got an increase of the heat load of about 1.5 W. The total measured heat load on the N bath is 6.6 W, corresponding to a hold time of 17 days in the laboratory. During the flight, the 1.5 W load from the window should be reduced by a factor at least 10, with a corresponding increase of the hold time.

3.5 External Plumbing

We need a system of valves and tubes (the plumbing) outside the cryostat. The main reason is that we need to pump on the He bath below the λ point for cycling the ^{3}He fridge at ground before the flight. After that we need to seal the He circuit, launch the payload, and re-open the He bath to the outer space once at float (external pressure $\sim$ 3 mbar). The sealed phase can be as long as 6 hours. During this phase the pressure of the He bath rises slowly but does not exceed 15 mbar. During pumpdown, the plumbing is used to fight development of Tacons oscillations. The plumbing has been built using 12 mm diameter bellows and high flow diaphragm valves (NUPRO-LD series). A schematics is shown in fig.4. The pumpdown is critical, and the development of Taconis oscillations must be monitored closely. Pressure oscillations in the fill and vent lines may produce an additional thermal input in the dewar. They are usually excited during pumpdown. We use a solid state pressure transducer (MPX7200A) with a differential amplifier connected to a wave analyzer to monitor pressure oscillations during pumpdown. The power spectrum of pressure in the He vent line, read by the MPX7200A, is a powerfull diagnostic tool and drives us in real time optimizing the valves configuration for pumping. The oscillations show up at a frequency of 1 - 20 Hz (depending on the pressure), with an amplitude which can be larger than 1 mbar rms. Acting on valves (3) (4) (5) (see fig.4) a fine tune is possible to reduce oscillations down to a negligible level. The pumpdown to $\sim$ 10 mmHg is done in about 20 hours. After that, the ^{3}He fridge is cycled. To seal the He bath during ascent and open it at float, we have motorized a copper gasket valve (MDC model MAV-150) using a gearbox DC motor (Globe Motors model A-1430-43A148-2) operated by telecommands. The nominal sealing torque is repeated over successive cycles, by electronically controlling the maximum current through the motor at closure.

3.6 Nitrogen Pressurization System

To prevent development of fluffy Nitrogen ice (float pressure is about 3 mbar), and loss of thermal contact between the cryogen and the cryostat tank, we developed a simple pressure control system for the Nitrogen tank. Nitrogen Vapours flow through three solenoid valves (which are mounted in parallel to reduce the flow impedance). The gas pressure is measured by a solid state absolute sensor (Motorola MPX7200A). The readout is amplified and compared to a trimmable reference level. The output of the comparator drives the solenoid valves. The system is trimmed to mantain the Nitrogen vapor pressure between 780 and 880 torr. The duty cycle of the system depends on the evaporation rate, on the tank volume free from liquid, and on the impedance of the vent line, including the three solenoid valves, and on the external pressure. We usually have a short ($\sim$ 1 minute) aperture of the solenoid valves every 15 minutes. These are mounted in parallel to reduce the flow impedance. A record of the Nitrogen pressure at float is shown in fig.5.

4. Test flight

The system has been flown on the BOOMERanG payload in two short flights, on Aug.12, 1997 and on Aug.30, 1997, from the National Scientific Balloon Facility of Palestine

(TX, USA). The cryostat survived the landing of the first flight (too short for cryogenic tests) and remained for 12 hours horizontal at ground, still mantaining Liquid Helium in the He tank. It was recovered and refilled, the ^{3}He fridge was recycled and the system was declared flight ready again in less than 10 days. In fig.6 we plot the He temperature during the second flight of Aug.30, 1997. During ascent the ^{4}He tank was sealed. Temperature of the ^{4}He bath rose to 2.05 K in three hours. Once at float the motorized valve was opened and the nominal 1.65 K in flight temperature was reached in four hours. The flight was terminated 0.5 hours later. The shields had not reached equilibrium at that point, but their temperature was raising fast above 12 K. The detectors temperature (0.3 K) drifted less than 5 mK during the 7.5 hours flight. A significant data set was obtained from the bolometric receivers. At the second landing the payload was dragged for about 200 m on rocks, and all the fill/vent lines were broken. The cryostat has been fixed and is now ready for the long duration balloon flight in Antarctica, scheduled for December 1998.

4. Conclusions

We have developed a He cryostat with a large (50 liters) volume available for the experiment and a long hold time ($> 12 days$). The system is suitable for Long Duration Ballooning. The system has been qualified in two mid-latitude balloon flights, and is now ready for the LDB flight.

5. Acknowledgments

This work has been supported by Programma Nazionale Ricerche in Antartide, Universita' di Roma La Sapienza and Agenzia Spaziale Italiana. We thank P. Mauskopf and A. Lange for discussions and suggestions during the design of the cryostat; E. Aquilini, B. Crill, and B. Netterfield for help in the measurements with the BOOMERanG cryostat; P. Mason for very helpful advice and support.

9. References

1) **Lange A., et al.** The BOOMERanG Experiment, Space Sci. Rev., **74**, 145-150, 1995.

2) **de Bernardis P. et al.** BOOMERanG: Balloon Observations Of Millimetric Extragalactic Radiation ANd Geophysics, in *Microwave Background Anisotropies*, F.R. Bouchet, R. Gispert, B. Guideroni, J. Tran Thanh Van editors, edition Frontiers, Gif sur Yvette, France, pg.155-160, 1997.

3) **Masi S. et al.** Measuring the Cosmic Microwave Background Anisotropy Power Spectrum using BOOMERanG, in *Topological Defects in Cosmology*, M. Signore, F. Melchiorri editors, World Scientific UK, 1998.

4) **Bock J., Chen P., Mauskopf P., Lange A.** A novel bolometer for infrared and millimeter-wave astrophysics, Space Sci. Rev., **74**, 229-235, 1995

5) **Mauskopf P., et al.** Composite infrared bolometers with Si_3N_4 micromesh absorbers, Applied Optics, **36**, 765-771, 1997.

6) **Masi S. et al.** A self contained ^{3}He refrigerator suitable for long duration balloon experiments, Cryogenics, in press, 1998.

7) **Palumbo P., et al.** Balloon-Borne ^{3}He cryostat for millimeter bolometric photometry, Cryogenics, (1994), **34**, 1001-1005.

8) **Astone P. et al.** The Gravitational Wave Detector Nautilus Operating at T $\sim$ 0.1 K, Astroparticle Physics, (1997), **7**, 231-243.

9) **Bellatreccia A., et al.** Superleak tigh aluminium to stainless steel bond, Cryogenics, (1983), **23**, 556-557.

10) **P.R. Roach**, Kevlar support for thermal insulation at low temperatures, Rev. Sci. Instrum., (1991), **63**, 3216-3217.

11) **L. Duband, L. Hui, A. Lange** Thermal isolation of large loads at low temperature using Kevlar rope, Cryogenics, (1993), **33**, 643-647

12) Zucchini A., Orsi R. Structural Calculations and Verifications of the Mechanical Support of a Space Cryogenic System, ENEA Report RT/INN/95/18, Frascati.

13) **A.B. Fradkov** Helium and Hydrogen Cryostats without Additional Liquid Nitrogen Cooling, Cryogenics, (1962), **2**, 177-179

14) **P. Lynam et al.** Reduction of the heat flux into liquid helium in wide necked metal dewars, Cryogenics, (1969), **9**, 242-246

15) **F.F. Mende et al.** Broad-neck helum cryostat with a long lifetime, Cryogenics, (1989), **29**, 998-1001

16) **J.F. Maguire, J.D. Ramsden, D.E. Wolman** Novel approach to supercritical helium flight cryostat support structures, Cryogenics, (1988), **28**, 142-146

17) **M. Murakami et al.** Design of cryogenic system for IRTS, Cryogenics, (1989), **29**, 553-558

18) **M. Murakami et al.** Thermal design and test of IRTS cryostat, Adv. Cryo. Eng. (1990), **35**, 295-302

19) **Bailey C.A.** Advanced Cryogenics (1971), 133-153, Plenum Press, London, 1971; **Bailey C.A. and Hands B.A.** Thermal Design (1986), in Cryogenic Engineering, Academic Press, London, 116-121.

20) **Jacobs S. et al.** Investigations into the thermal performance of multilayer insulation (300 - 77 K), Cryogenics, (1992), **32**, 1137-1153

21) **Cheng G.** Performance of Multilayer Insulation with slotted shield Cryogenics, (1994), **34**, 381-384.

22) Kevlar is a trade mark of DuPont corporation. Cortland Cable Company, Cortland, N.Y. (USA).

23) Meccano SpA, Centro per l' Innovazione Tecnologica, Fabriano, Italy.

24) Cryolam NRC-2, Metallized Products, Inc., Winchester, MA, (USA)

External height	1565 mm
External diameter	802 mm
Experimental space (height)	700 mm
Experimental space (diameter)	345 mm
Weight	∼250 Kg
Nitrogen tank volume	∼75 liters
Helium tank volume	∼65 liters
Hold time	up to 17 days
Serpentine lenght	11 m
Serpentine diameter	8 mm
Fill/vent tubes diameter	1/2 inch
Fill/vent tubes thickness	8 mil
Suspension system	Kevlar cord, 1.65 mm dia
Windows	2, each 76 mm dia
Window material	polypropylene (50 μm thick)

Table 1: Main specifications of the cryostat

Efficiency	Shield temperature (K)	Heat Load (mW)
0.1	50	152
0.2	37	102
0.3	31	80
0.4	28	70
0.5	26	63
0.6	23	56
0.7	21	54
0.8	20	52
0.9	18	49
1.0	17	48

Table 2: Results of the thermal model for the vapour cooled shield. The shield temperature and the resulting heat load on the He tank are computed for different values of the heat exchange efficiency for the vapours flowing in the serpentine and in the heat exchanger on the shield.

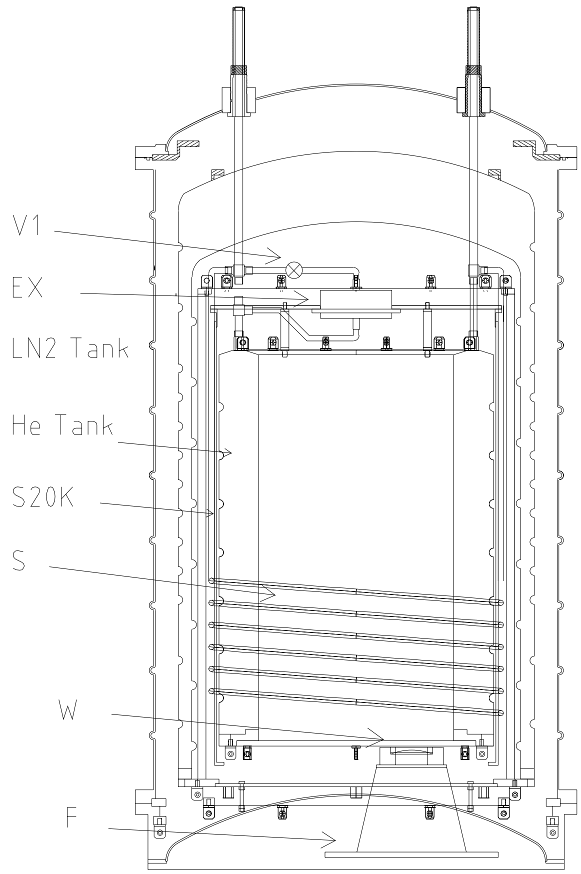

Fig 1

Figure 1: Section of the cryostat. The main parts are labeled as follows: N: Nitrogen tank; He: Helium tank; FI: He fill line; VE: He vent line; V1: motorized valve in the internal plumbing; EX: He vapour-shield heat exchanger; S20K: vapour cooled shield; S: serpentine; W: window; F: funnel.

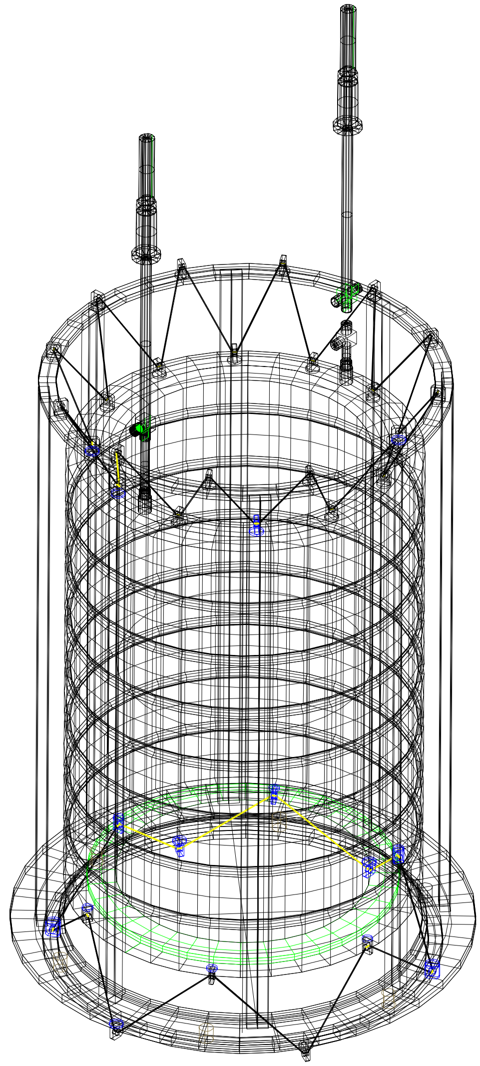

Figure 2: A: The He tank and the support system based on kevlar ropes.

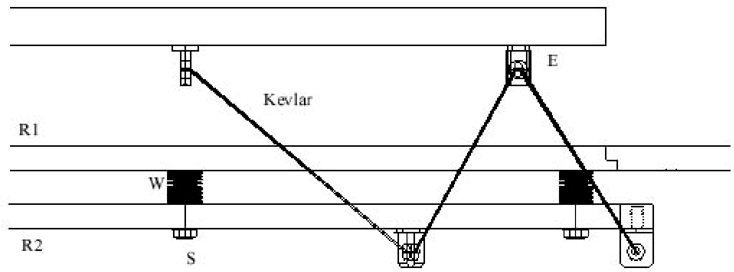

Fig 2B

Figure 2: B: concept drawing of the kevlar tensioning system.

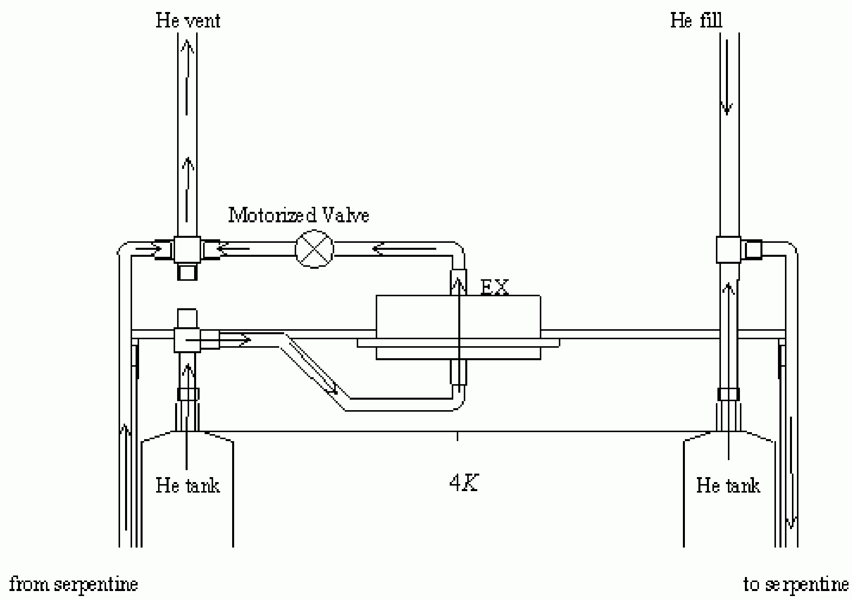

Fig 3

Figure 3: Internal plumbing for the He evaporation and control of shield temperature.

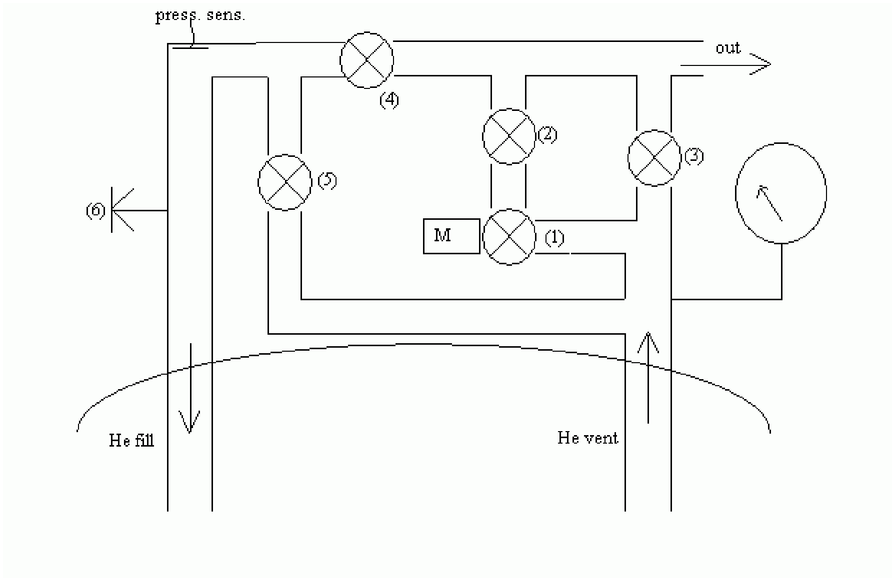

Fig 4

Figure 4: Schematics of the external plumbing for Helium. The He tank has separate fill and vent tubes. During normal operation the vapours flow through the vent line. Before launch and during ascent valves (1),(3),(4),(5) are closed, and valve (2) is open. Pressure drifts slowly up. Once at float, a command opens valve (1), thus restoring pumping, down to the external pressure (about 3 mbar). Valve (3) is a bypass used in the lab for the motorized valve (1). Valve (2) is used to shut the line to the motorized valve. Valve (4) is to vent through the fill line (e.g. during transfer and during pumpdown). Valve (5) is a bypass used to control pressure oscillations during pumpdown. Before separation a command closes valve (1). After landing, when pressure is high enough, Helium can flow out through the relief valve (6).

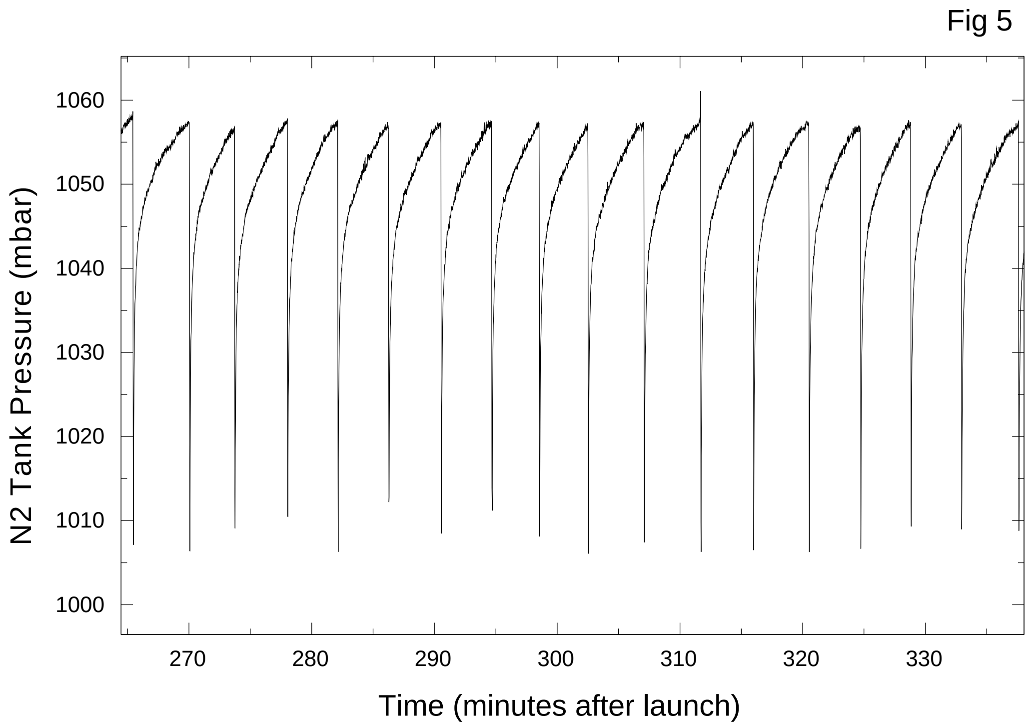

Figure 5: Pressure of the liquid nitrogen bath during the flight of Aug.30, 1997. The pressure was controlled by solenoid valves to avoid the formation of solid nitrogen in the tank.

Fig 6

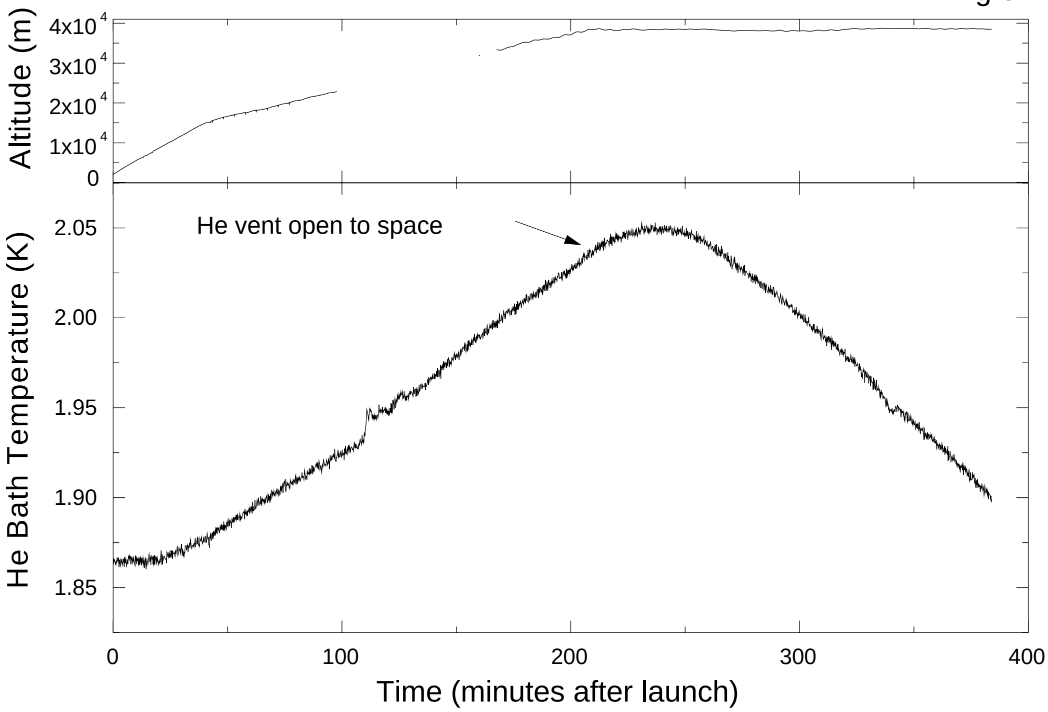

Figure 6: Temperature of He bath inside the cryostat during the flight of the payload BOOMERanG on Aug.30, 1997 (bottom panel). In the top panel the altitude of the payload is plotted. The He bath was sealed closing the motorized valve (1), which was re-opened at float, at an external pressure of 3 mbar. At the end of the flight the He bath was sealed again to avoid ice plugs during fall in the atmosphere and landing.